Characteristics of bistable localized emission states in broad-area vertical-cavity surface-emitting lasers with frequency-selective feedback

Y. Tanguy and T. Ackemann*
SUPA, Department of Physics, University of Strathclyde, 107 Rottenrow, Glasgow G4 0NG, Scotland, United Kingdom

R. Jäger
ULM Photonics, Lise-Meitner-Str. 13, 89081 Ulm, Germany

(Received 16 May 2006; published 30 November 2006)

Small-area bistable lasing spots (about 10 μm full width at half maximum) can be created at different positions within the aperture of a broad-area vertical-cavity surface-emitting laser (aperture diameter 80 μm) with frequency-selective feedback from a grating in Littrow configuration, and an additional pinhole localizing feedback to a part of the laser. Their characteristics are analyzed depending on the grating tuning, injection current, and feedback strength. These spots are considered to be good candidates for self-localized cavity solitons, if the perturbation by boundaries can be reduced using devices with larger diameter.

DOI: 10.1103/PhysRevA.74.053824 PACS number(s): 42.55.Px, 42.65.Pc, 42.65.Tg

Recent years showed remarkable progress in achieving, controlling, and understanding of bistable solitonlike emission states, which are usually referred to as *cavity solitons* (CS), in semiconductor microcavities (see, e.g. [1–3] for recent reviews). They are discussed as "bits" for future all-optically and potentially massively parallel information processing schemes. Currently realized schemes rely on a passive (i.e., absorbing, e.g. [4]) or active (i.e., amplifying [5,6]) semiconductor microcavity driven by a broad-area holding beam of high spatial and temporal coherence. The detuning between the frequency of the injected field and the cavity resonance is a critical parameter. Recently, this work was extended to the case of a laser with injected signal [7,8], i.e., a situation where the free-running cavity is above threshold. However, these schemes still need a coherent driving field.

For applications, devices should be cascadable, compact, and as simple as possible. Hence it appears to be advantageous to remove the necessity of a broad-area holding beam and to supply the energy purely by incoherent means, i.e., electrical pumping or optical pumping with low-coherence light sources. A device like this with self-sustained localized emission states might be called a *cavity soliton laser* (CSL).

There are several reports in the literature on cavity soliton lasers in nonsemiconductor lasers or photorefractive oscillators [9–12] and there is also significant theoretical coverage, e.g. [3,11,13]. These authors incorporated saturable absorbers into the laser cavity favoring bistable operation characteristics. Recently, the possibility of CS in semiconductor-based lasers with saturable absorbers was addressed [14].

We are following a different approach and investigate a vertical-cavity surface-emitting laser (VCSEL) with frequency-selective feedback as a candidate for a CSL. This is motivated by the recent observation of an abrupt turn-on behavior accompanied by hysteresis in such a system [15]. The theoretical analysis shows that the system exhibits the possibility of a bistability between the nonlasing off state and lasing states (in a model without spatial degrees of freedom). In line with observations done in lasers with saturable absorbers and general considerations on the properties of cavity solitons (see the reviews mentioned above), this might provide the basis for CS formation in lasers with frequency-selective feedback.

The experiment utilizes a broad-area bottom-emitting VCSEL with an emission wavelength at 980 nm (similar to the ones described in [16]). It is electrically pumped through an 80 μm circular oxide aperture. The experimental apparatus is shown in Fig. 1. The external cavity included an aspheric collimator (f=8 mm, NA 0.5), a half-wave plate, a planoconvex lens with f=300 mm, and a holographic grating (1800 lines/mm) in the Littrow configuration. The external cavity is in a self-imaging condition and its length is about 62 cm. An intracavity beam splitter couples out about 1% of

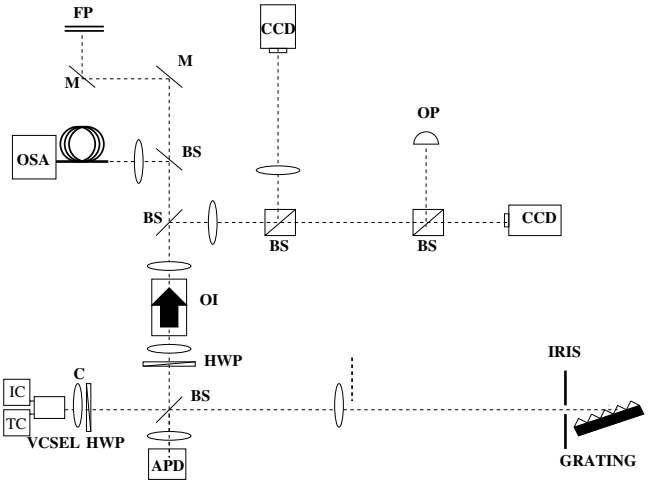

FIG. 1. Experimental apparatus. The self-imaging external cavity consists of a 8 mm aspherical lens (C), a 300 mm lens, and a holographic grating (1800 lines/mm). A beam sampler is also inserted to couple out part of the beam for the detection part. OI: optical isolator; M: mirror; CCD: camera; BS: beam sampler or beam splitter; OP: photodiode; FP: scanning Fabry-Pérot; OSA: optical spectrum analyzer.

*Email address: thorsten.ackemann@strath.ac.uk

the beam (for horizontal polarization) into the detection part. The diffraction efficiency differs strongly for the two polarization components (a ratio of 1 to 20 favoring the horizontal polarization; see also [15,17]). The main principal axis of the VCSEL is aligned with the preferred axis of the grating using the half-wave plate.

The intensity distributions of the VCSEL in the near field and far field are monitored by CCD cameras and its optical spectrum by both an optical spectrum analyzer (HP 86140*A*) and two scanning Fabry-Pérot interferometers with different free spectral range.

Beam propagation within the self-imaging cavity was modeled using the formalism of 3×3*ABCDEF* transfer matrices [18]. For a given angular alignment of the grating, rays with a certain frequency (referred to as "grating frequency" in the following) form closed loops in the external cavity irrespective of their location and angle. If the emission wavelength deviates from the grating wavelength the reentering rays still arrive at the original position but with an incorrect angle. From the angular dispersion (0.15 rad/nm) and the angular width of the VCSEL resonance (about 0.026 rad estimated from mirror reflectivities typical for VCSELs), the bandwidth of the feedback in frequency space is estimated to be around 55 GHz. This encompasses many longitudinal modes of the external cavity which have a free spectral range of 250 MHz.

First, the behavior of the solitary laser was analyzed. Due to an inhomogeneous current spreading inherent to the construction of electrically pumped VCSELs (e.g. [5,16]), lasing emission at threshold is confined to the perimeter of the device. The dominant transverse wave number of this emission increases like the square root of the detuning from the emission from the longitudinal cavity resonance. It can be tuned by varying the temperature because this changes the offset between the gain maximum and the cavity resonance [19,20]. A detailed experimental and theoretical investigation was recently done for square VCSELS [20].

In the next step, the optical feedback from the grating was carefully aligned, in particular by adjusting the reimaged far-field angles. The grating frequency was chosen to coincide approximately with the longitudinal resonance of the VCSEL cavity below the solitary laser threshold. A 50% threshold reduction was measured, with on-axis lasing emission starting on the edges. At higher injection current, lasing emission is also present closer to the center of the aperture. In particular, a bright spot was observed, which showed hysteresis, if the current was ramped up and down. However, the observation of this bistable spot depended critically on parameters, which was ascribed to perturbative effects from optical structures in the background and at the perimeter.

As a consequence an aperture was introduced into the cavity in order to shut off feedback and inhibit lasing at the boundaries. The iris was positioned on a *x*-*y* translation stage as close as possible to the grating, where the near field is reimaged. The diameter of the iris was adjusted such that feedback is only present in a 25 μm area of the near field. Under these conditions, bistable spots are a robust phenomenon and were obtained in at least four different locations in the near field, one at a time, depending on the position of the iris. Figure 2 displays two of these spots. These localized

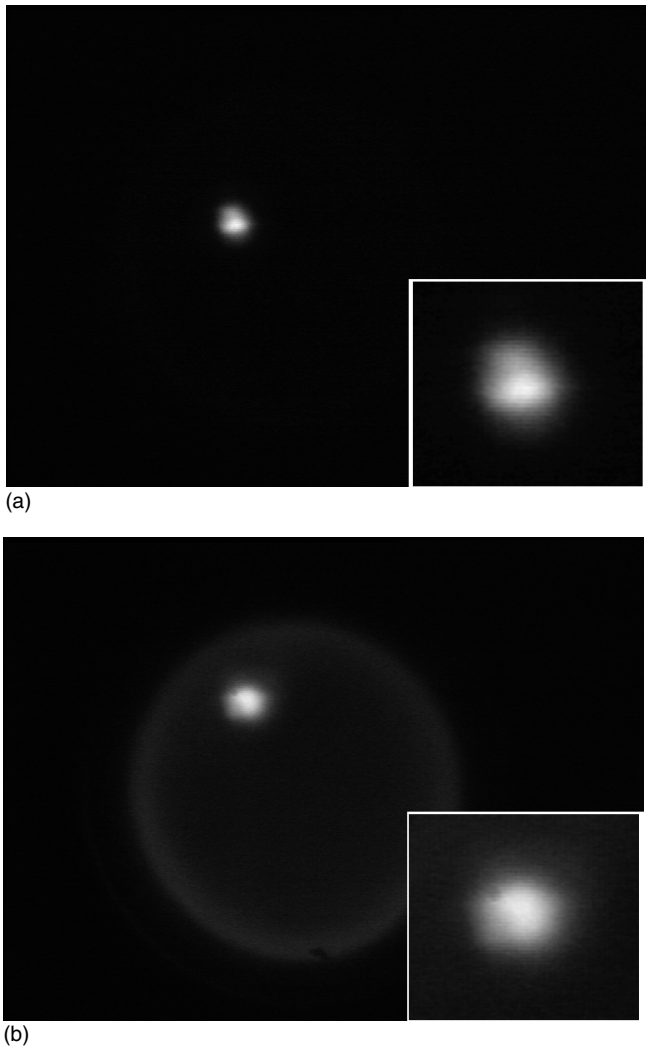

FIG. 2. Bistable spots in near field obtained for different positions of the filtering aperture. Top (bottom) picture with current at 49.2 mA (46.6 mA) and device temperature 13 °C. Insets display close-ups of the spots. In the right image, the spontaneous emission originating from the perimeter of the laser can be distinguished.

emission states have a full width of 10 μm at the $1/e^2$ point, i.e., are substantially smaller than the aperture. Because of the strong anisotropy of the diffraction efficiency of the grating, these spots are all linearly polarized in the horizontal plane.

The spectra of the spots were recorded with a scanning confocal Fabry-Pérot. The spot operated either on a single or multilongitudinal modes, depending on the injection current. The linewidth was measured to be 2.5 MHz. This is in accordance with typical linewidths (on the millisecond time scale) known from grating-controlled semiconductor lasers and illustrates that these spots seem to be small lasers. The mechanisms of their stabilization need to be clarified further in the future. We cannot conclude on self-localization and hence ascribe a solitonic character to them, because obviously a combination of boundary-induced localization (due to the aperture) and seeding by local inhomogeneities in the active layer or the cavity also plays a role. The latter is inferred from the fact that bistable spots could not be ob-

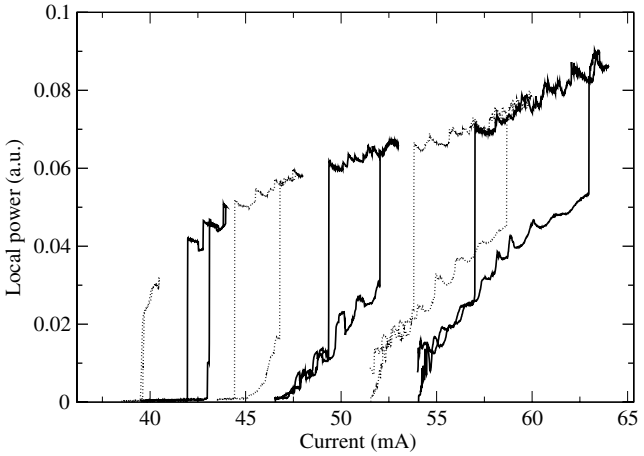

FIG. 3. LI curves for different grating angles. The grating wavelength is increasing over a 0.3 nm range, with corresponding bistability curves (six of them) from left to right. The device temperature is kept constant at 13 °C. For these experiments, the external cavity contained an additional blade to partially remove feedback for off-axis waves.

tained at all locations within the transverse aperture.

Light-intensity (LI) curves from a bistable spot are shown in Fig. 3, each curve corresponding to a different grating angle over a 0.3 nm range. If the detuning (frequency of solitary laser minus grating frequency) is increased, the threshold increases, the hysteresis loop widens, and the total intensity increases. Whereas the latter is obviously related to the higher gain at higher injection current, the shift of threshold seems to be mainly related to the thermal tuning of the cavity resonance of the free-running laser. The change of threshold versus grating frequency corresponds well to the previously measured detuning of the solitary laser on-axis beam with current (0.014 nm/mA), indicating that at the threshold for bistability the actual detuning is approximately constant.

We also note that for the bistability curves with higher thresholds the local intensity is already nonzero before the spot turns on. Experimental near-field pictures (not shown) taken before the spot turn-on show off-axis emission patterns located mainly between the area with the spot and the device boundary. These off-axis beams are blue detuned with respect to the grating frequency. They could be removed partially by introducing an additional filter (a blade) in the feedback loop. This was positioned after the 300 mm lens, where the spatial separation is maximum between beams of different wavelengths. Without this additional filtering all LI curves displayed a nonzero intensity before the spot switches on. Possibly, this is connected to the fact that besides the optimum feedback condition we mentioned so far (closed paths at the grating frequency), there are also combinations of angles and frequencies for which the beam is exactly retroreflected by the grating. This implies that a ray with a transverse wave vector $\vec{k}_\perp$ has a wave vector $-\vec{k}_\perp$ after a round trip in the external cavity. Since wave vectors can be coupled by reflections at the boundary in the VCSEL (and by nonlinearities, e.g. [21]), this might explain the excitation of the background waves, especially taking into account the finite angular and spectral resonance width of the VCSEL.

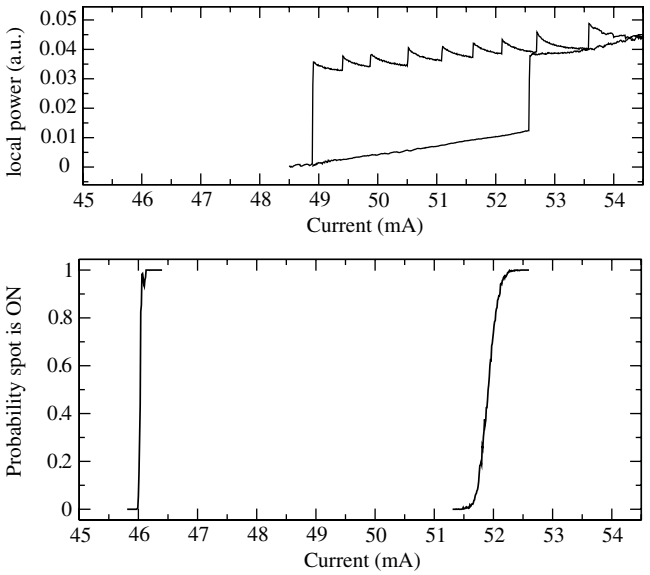

FIG. 4. Top picture: LI curve showing the hysteresis range of a localized emission. Bottom picture: Probability of obtaining the state with the spot switched on, after cutting the feedback loop with the optical chopper. The two curves correspond to the two different directions of the wheel rotation. For this particular experiment a grating with 1200 g/mm was employed.

The upper portion of the LI curves displayed in Fig. 3 (see also the upper part of Fig. 4) shows typically some sawtooth-like modulations. These are related to sudden frequency shifts of the emission corresponding to the transition between different longitudinal modes. Similar observations were done in other semiconductor lasers with frequency-selective feedback [22,23]. The abrupt switch off of the spot occurs at such a transition, and hence limits the hysteresis range. The hysteresis range was investigated in more detail by placing an optical chopper in the external cavity, cutting and opening repetitively the feedback loop, and monitoring which state (spot on or off) is found after a transient. Figure 4 shows a histogram of the data, the value denoting the fraction of events in which the spot was found. The resulting curves are typical for bistable systems showing a smooth transition between the two limiting cases in which one or the other branch is much more stable and hence attractive for most initial conditions. Surprisingly, the statistics depend on the direction of rotation of the chopper. In one case, the transition is very close to the right-hand side of the hysteresis, in agreement with the fact that the system switches on spontaneously for slightly higher current. In the other case, the on state is still reached for much lower current values, beyond the point where spontaneous switch off occurs. This illustrates that lasing states exist at much lower current values than indicated by the hysteresis loop. This is in agreement with the calculations reported in [15] for a VCSEL with frequency-selective feedback, where the hysteresis width in simulated LI curves was always smaller than the coexistence range between the lasing and the nonlasing solutions obtained from analytical calculations. Probably, they can be accessed for particular operation conditions stemming from

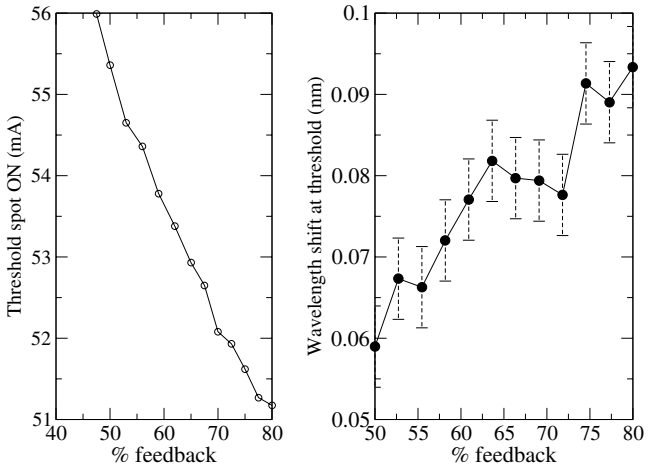

FIG. 5. Bistability thresholds and associated frequency shifts vs feedback strength. Device temperature 13 °C.

the interaction with the background off-axis waves (see the discussion above), which is different for the different direction of rotation of the chopper wheel.

In an additional experiment we varied the feedback strength, keeping a constant grating angle. In order to do so, a polarizer and a half wave plate were inserted in the external cavity. Taking advantage of the strong anisotropic grating feedback efficiency, the feedback strength could be adjusted between 80 to 4%. The resulting bistability thresholds and associated frequency shifts are plotted in Fig. 5. The bistability threshold increases monotonously (and nearly linearly) with decreasing feedback strength. Below 45% of feedback strength bistability could not be obtained. The frequency shift displayed is the shift between the low-amplitude precursor and the high-amplitude spot and increases with increasing feedback. Its origin can be understood by considering the origin of bistability in lasers with frequency-selective feedback.

This mechanism was investigated in a model without spatial degrees of freedom [15]. Due to the phase-amplitude coupling in semiconductor lasers (described in the simplest case by the linewidth-enhancement factor or α factor [24]), a decrease in carrier density will cause a redshift of the cavity resonance. In the case of a positive detuning between the VCSEL cavity resonance and the grating frequency, this phase-amplitude coupling effect shifts the emission frequency closer to the optimum feedback frequency, which further increases the feedback strength. This depletes the carrier density and enhances the effect, ending in an abrupt lasing turn on. The thermal frequency shift with increasing current contributes to initiating this self-amplifying phenomenon due to the reduction in detuning. The frequency shift displayed in Fig. 5 is the one associated with the jump of emission from the free-running or spontaneous emission condition to the grating controlled regime [15,25]. Obviously the mechanism is also compatible with the observation displayed in Fig. 3 for the shift of the LI curves with current and grating frequency.

In summary, we analyzed the properties of bistable small-area lasing spots in a broad-area VCSEL with frequency-selective feedback. Presently, localization is facilitated by the aperture needed to filter out perturbing effects from nearby boundaries. It is hoped that in a device with a larger area, these effects can be minimized and true self-localized cavity solitons become accessible.

We are grateful to several colleagues who contributed by useful discussions or to preliminary experimental stages of this work: W. J. Firth, F. Papoff, X. Hachair, M. Giudici, and in particular J. R. Tredicce, A. Naumenko, N. A. Loiko, M. Sondermann, M. Schulz-Ruhtenberg, and M. Marino. This work was supported by the European Union within the FunFACS project and a starter grant by the Faculty of Science of the University of Strathclyde.

[1] W. J. Firth and C. O. Weiss, Opt. Photonics News **13**, 54 (2002).
[2] L. A. Lugiato, IEEE J. Quantum Electron. **39**, 193 (2003).
[3] *Dissipative Solitons*, edited by N. Akhmediev and A. Ankiewicz, Lecture Notes in Physics Vol. 661 (Springer, New York, 2005).
[4] V. B. Taranenko and C. O. Weiss, Appl. Phys. B: Lasers Opt. **72**, 893 (2001).
[5] S. Barland *et al.*, Nature (London) **419**, 699 (2002).
[6] S. Barbay, Y. Ménesguen, X. Hachair, L. Leroy, I. Sagnes, and R. Kuszelewicz, Opt. Lett. **31**, 1504 (2006).
[7] Y. Larionova and C. Weiss, Opt. Express **13**, 10711 (2005).
[8] X. Hachair *et al.*, IEEE J. Sel. Top. Quantum Electron. **12**, 339 (2006).
[9] V. Y. Bazhenov, V. B. Taranenko, and M. V. Vasnetsov, Proc. SPIE **1840**, 183 (1992).
[10] M. Saffman, D. Montgomery, and D. Z. Anderson, Opt. Lett. **19**, 518 (1994).
[11] V. B. Taranenko, K. Staliunas, and C. O. Weiss, Phys. Rev. A **56**, 1582 (1997).
[12] C. O. Weiss, M. Vaupel, K. Staliunas, G. Slekys, and V. B. Taranenko, Appl. Phys. B: Lasers Opt. **68**, 151 (1999).
[13] N. N. Rosanov, *Spatial Hysteresis and Optical Patterns*, Springer Series in Synergetics (Springer, Berlin, 2002).
[14] M. Bache, F. Prati, G. Tissoni, R. Kheradmand, L. A. Lugiato, I. Protsenko, and M. Brambilla, Appl. Phys. B **81**, 913 (2005).
[15] A. Naumenko, N. A. Loiko, M. Sondermann, K. F. Jentsch, and T. Ackemann, Opt. Commun. **259**, 823 (2006).
[16] M. Grabherr, M. Miller, R. Jäger, R. Michalzik, U. Martin, H. J. Unold, and K. J. Ebeling, IEEE J. Sel. Top. Quantum Electron. **5**, 495 (1999).
[17] F. Marino, S. Barland, and S. Balle, IEEE Photon. Technol. Lett. **15**, 789 (2003).
[18] O. Martinez, IEEE J. Quantum Electron. **24**, 2530 (1988).
[19] S. P. Hegarty, G. Huyet, J. G. McInerney, and K. D. Choquette, Phys. Rev. Lett. **82**, 1434 (1999).

[20] I. Schulz-Ruhtenberg, M. Babushkin, T. Loiko, N. A. Ackemann, and K. F. Huang, Appl. Phys. B: Lasers Opt. **81**, 945 (2005).
[21] I. V. Babushkin, N. A. Loiko, and T. Ackemann, Phys. Rev. A **67**, 013813 (2003).
[22] A. V. Naumenko, P. Besnard, N. A. Loiko, G. Ughetto, and J. C. Bertreux, IEEE J. Quantum Electron. **39**, 1216 (2003).
[23] A. P. A. Fischer, O. K. Andersen, M. Yousefi, S. Stolte, and D. Lenstra, IEEE J. Quantum Electron. **36**, 375 (2000).
[24] C. H. Henry, IEEE J. Quantum Electron. **18**, 259 (1982).
[25] M. Giudici, L. Giuggioli, C. Green, and J. R. Tredicce, Chaos, Solitons Fractals **10**, 811 (1999).